Stability of Superconducting Wire With Various Surface Conditions in Pressurized He II (2)—Numerical Analysis

S. Shigemasu, M. Ohya, Y. Shirai, M. Shiotsu, and S. Imagawa

Abstract—**We developed a computer code to analyze the stability of a superconducting wire in He II based on the one-dimensional heat equation. We applied to this code our experimental data on heat transfer characteristics of He II, such as Kapitza conductance, critical heat flux and heat transfer curve in film boiling. Using this code, we simulated the recovery or quench process of a normal zone that was initiated by a thermal disturbance for the liquid helium temperatures from 1.8 K to 2.0 K at atmospheric pressure. The numerical solutions agreed with our experimental data for the same characteristics of the wire (bare and oxidized surfaces) and corresponding experimental conditions. We clarified the influences of the surface insulation and the liquid helium temperature on the stability of the superconducting wire.**

Index Terms—**Kapitza conductance, stability, superfluid helium.**

I. INTRODUCTION

I T IS KNOWN that the performance of a superconducting magnet is improved by cooling in He II. The heat transfer from a conductor surface to He II is dominated by Kapitza conductance [1], [2]. The electrical insulation of a superconducting wire constitutes Kapitza conductance between the surface of the wire and He II, and may influence the stability of the superconducting wire cooled by He II. The heat transfer characteristics like Kapitza conductance can be an important factor in the analysis of the stability. However, only a few numbers of numerical analyses were accounting for these characteristics. We developed and performed a computer code to analyze the stability of a superconducting wire in He II based on the one-dimensional heat equation.

This paper describes the analysis of the stability and the comparison with the experimental data presented in part (1) of this paper [3]. Then we clarify the influences of the surface insulation on the stability of the superconducting wire.

II. NUMERICAL ANALYSIS

A. Analytical Model

We analyzed the stability of a superconducting wire in the same condition as the experiment. The parameters of wires and

TABLE I
PARAMETER OF WIRES AND METHODS

	Experiment		Analysis	
	Wire-A	Wire-B	Wire-A	Wire-B
Wire Surface	Bare	Oxidized	Bare	Oxidized
Wire Diameter (mm)	0.50	0.50	0.50	0.50
Cu/NbTi	1.3	1.3	1.3	1.3
Heater Width (mm)	10	20	10	20
Heat Input (mJ)	40.2	68.0	40.2	68.0
Heater pulse width (ms)	20	20	20	20

methods are listed in Table I. The analytical object and thermal phenomenon are symmetrical about the middle of the heater so that we analyze only half of a wire. The length from the middle of the heater to the end of a wire in the analysis is 100 mm, which is sufficiently long in as much that the temperature of the wire end can be regarded as the bath temperature.

B. Fundamental Equations

One-dimensional heat balance for the wire is described by the following equation.

$$C(B,T)\frac{\partial T}{\partial t} = \frac{\partial}{\partial x}\left\{\overline{\lambda}(B,T)\frac{\partial T}{\partial x}\right\} + Q_h + Q_j - Q_c \quad (1)$$

where x is the length from the middle of the wire; t is the time; T is the temperature. The heat capacity C and the average thermal conductivity $\overline{\lambda}$ of the wire are described as

$$\begin{cases} C(B,T) = C_{Cu}(B,T) \\ \overline{\lambda}(B,T) = \frac{f}{1+f}\lambda_{Cu}(B,T) \end{cases} \quad (2)$$

where f is Cu/NbTi ratio. The thermal capacities of the copper and NbTi are almost in the same order at helium temperature so that C is substituted for that of the copper. The thermal conductivity of NbTi is much less than that of copper so that $\overline{\lambda}$ is substituted for that of the copper, considering the cross sectional ratio. C and $\overline{\lambda}$ are the function of temperature T and magnetic flux density B.

Q_h is the heat power density that is heater power divided by the volume of the heater section.

Q_j is the Joule heating per unit volume. We consider temperature of a cross section in the wire as constant, so we approximate Q_j as

$$Q_j = \frac{\overline{\rho}(B,T)I^2}{S^2} \qquad (3)$$

where I is current; S is the cross section of the wire. $\overline{\rho}$ is the average resistivity of the superconducting wire and is expressed as

$$\overline{\rho} = \frac{S}{\frac{S_f}{\rho_f} + \frac{S_{Cu}}{\rho_{Cu}}} = \frac{\rho_f \rho_{Cu} S}{\rho_{Cu} S_f + \rho_f S_{Cu}} \qquad (4)$$

where ρ_f and ρ_{Cu} is the resistivity of NbTi and the copper respectively; S_f is the cross section of NbTi and S_{Cu} is that of the copper. ρ_{Cu} is also considered as a function of the influences of the temperature and the magnetic flux density. ρ_f is expressed as

$$\rho_f = \begin{cases} 0 & (T < T_{sc}) \\ \frac{B}{B_c}\left(1 + \frac{B}{2B_c}\right)^{-1}\frac{I - I_c}{I}\rho_N & (T_{sc} \le T < T_c) \\ \rho_N & (T_c \le T) \end{cases} \qquad (5)$$

where T_{sc} is the current sharing temperature of the wire; T_c, B_c and I_c are the critical temperature, the critical magnetic field density and the critical temperature of the wire, respectively; ρ_N is the normal resistivity of NbTi.

In the nonboiling regime, Q_c on each wire is described by the upper one of (6),

$$Q_c = \begin{cases} \alpha\left(T^n - T_b^n\right) \times \frac{P}{S} & (nonboiling \ regime) \\ q_{cr} \times \frac{P}{S} & (film \ boiling \ regime) \end{cases} \qquad (6)$$

where T_b is the bath temperature. P is the cooling perimeter, which is taken to be 67% simulating the experimental set up of the superconductor in a groove [3]. The coefficient α and the exponent n depend on the wire surface material and condition. They are taken to be $\alpha = 701$ and $n = 3.00$ for wire-A with bare surface and $\alpha = 203$ and $n = 2.86$ for wire-B with oxidized surface as reported by Iwamoto, *et al.* [4]. Q_c is converted to the heat quantity per unit volume by the term P/S. In the film boiling regime, we regard the heat flux as the constant value per unit volume as shown in the lower one of (6), where the critical heat flux q_{cr} is given by (7) [5],

$$q_{cr} = 0.58 \times \left\{ \frac{2}{r} \int_{T_b}^{T_\lambda} f(T)^{-1} dT \right\}^{\frac{1}{3}}$$

$$f(T)^{-1} = \frac{\rho^{*2} s_\lambda^4 T_\lambda^3}{A} \left\{ \left(\frac{T}{T_\lambda}\right)^{6.8} \left(1 - \left(\frac{T}{T_\lambda}\right)^{6.8}\right) \right\}^3 \qquad (7)$$

where T_λ is the lambda temperature; ρ^* is the density of He II; s_λ is the entropy at the lambda temperature; A is the Gorter-Mellink parameter.

C. Numerical Analysis Procedure

The numerical analyses were performed according to the following procedure. The dimension of a grid is 1.0 mm and time integration was performed explicitly with time step of 1.0×10^{-6} s. At first, we consider a wire immersed in He II. We set I, T_b, B on the wire. Both ends ($x = 0$ mm and 100 mm) are set as adiabatic. From these conditions, the critical temperature and the critical heat flux are determined. In each time step, the wire temperature is calculated by solving (1). This process is repeated until the wire temperature keeps a constant value or a part of the wire temperature exceeds 150 K. Bath temperatures are 1.8 K and 2.0 K at atmospheric pressure, and magnetic flux densities ranged from 1.2 T to 8 T. The magnetic flux density is regarded as constant in the analytical system.

III. RESULTS AND DISCUSSION

A. Example of the Numerical Data

The profiles of temperature with respect to the space and time for $T_b = 2.0$ K under a magnetic field of 4 T are shown in Figs. 1(a)–(c). The results are classified into three groups depending on the magnetic flux density and the test wire current.

(Group I) Fig. 1(a) shows the profile for $I = 100$ A. As shown in the figure, the temperature near the heater rises and the normal zone arises just after the addition of a step heat input to the heater at $t = 0$. The heater power is shut off at $t = 20$ ms. Then, the temperature near the section decreases and the wire recovers to the superconducting state.

(Group II) Fig. 1(b) shows the profile for $I = 130$ A. As shown in the figure, the normal zone is generated near the heater section at the start of step heating at $t = 0$ similar to Fig. 1(a). However, the wire doesn't recover to the superconducting state after the heater power shut off at $t = 20$ ms. At this time the wire temperature near the heater has reached about 7 K that is higher than the critical temperature for the NbTi under 4 T of 5.77 K, so the normal zone remains.

(Group III) Fig. 1(c) shows the profile for $I = 160$ A. As shown in the figure, the temperature near the heater section keeps increasing after the heater power is shut off. The higher temperature part of the wire is cooled by film boiling.

Fig. 2 shows the numerical results classified into these three groups on the graph of test current versus magnetic flux density. We define the minimum current belonging to Group II as I_R, and the minimum current belonging to Group III as I_F. The curves expressing the I_R and I_F are shown in the graph.

B. Comparison With the Experimental Data

Figs. 3(a)–(b) show the comparisons of the numerical results with the experimental data reported in part (1) of this paper [3] for the wire-A and wire-B, respectively. The experimental data of I_F are plotted by using double circles and double triangles for 1.8 K and 2.0 K, respectively. And the experimental data of I_R are plotted by using circles and triangles for 1.8 K and 2.0 K, respectively. The numerically obtained limit currents at 1.8 K and 2.0 K are shown as the solid lines and the broken lines. As shown in the figure, the numerical solutions are in good agreement with the experimental data within 16% errors (wire-A) and 10% errors (wire-B). It was confirmed that the physical phenomenon was well described by the model.
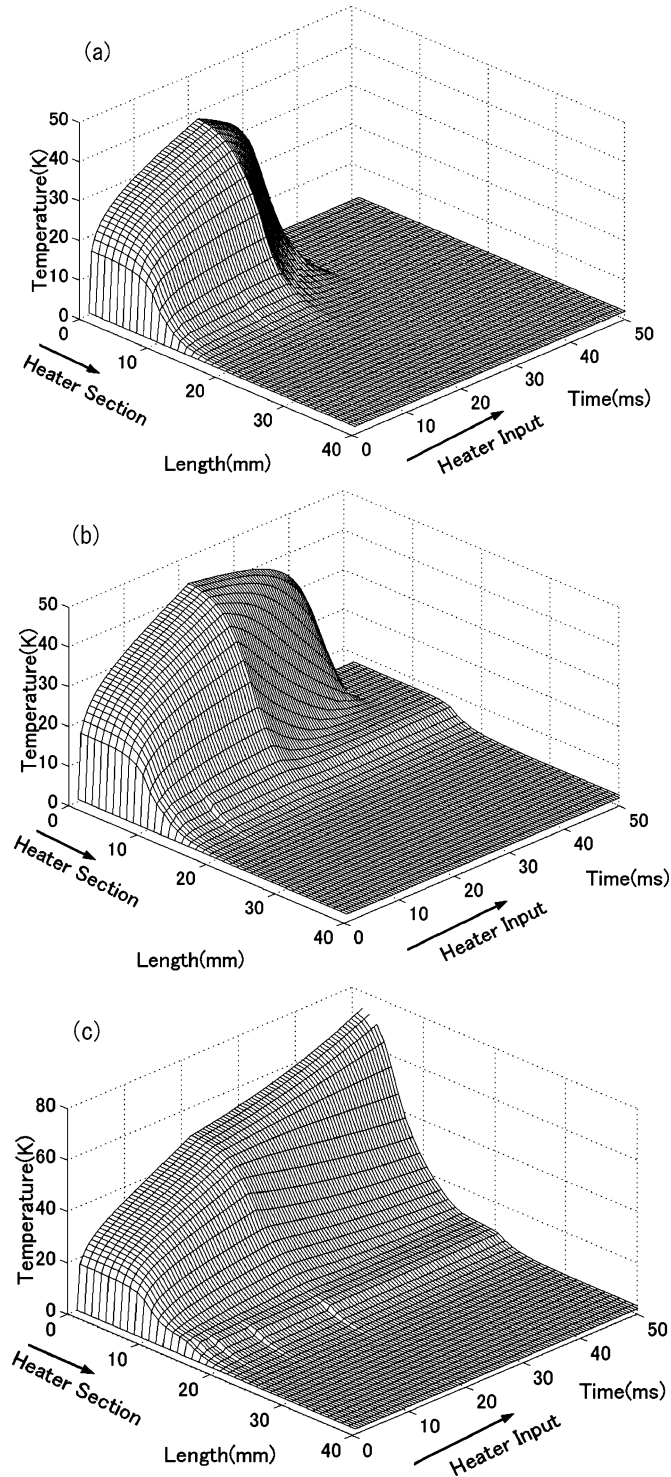
Fig. 1. Calculation results for the wire-B (a) $T_b = 2.0$ K, $B = 4$ T, $I = 100$ A (b) $T_b = 2.0$ K, $B = 4$ T, $I = 130$ A (c) $T_b = 2.0$ K, $B = 4$ T, $I = 160$ A.
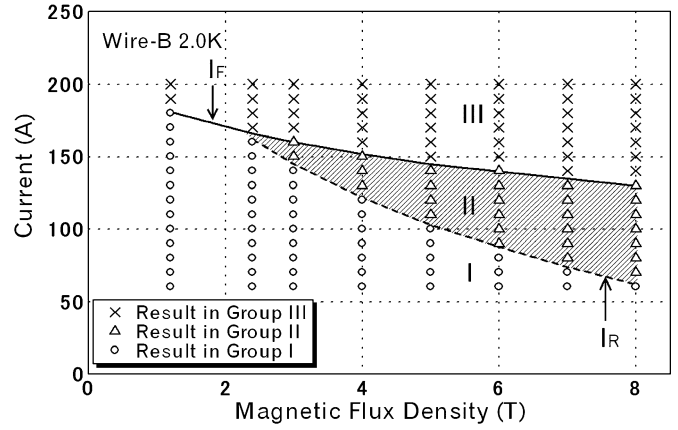

Fig. 2. Classification of the three groups for wire-B at 2.0 K.
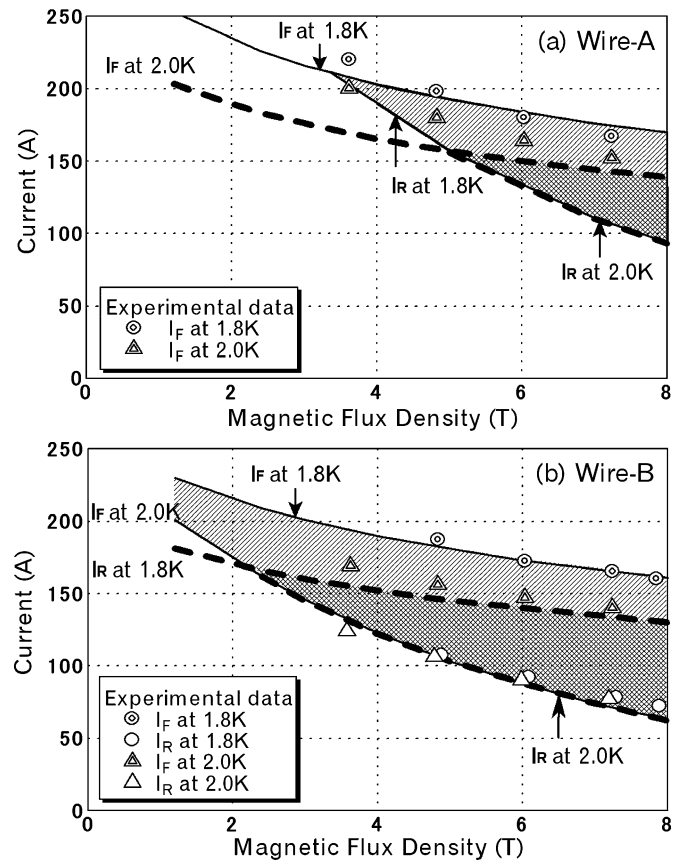
Fig. 3. Comparison of the numerical data with the experimental data of (a) wire-A (b) wire-B.

C. Discussion

To be the Group I or Group II depends on the nonboiling heat transfer for the wire in He II governed by Kapitza conductance and the critical temperature of the wire. Fig. 4 shows how the classification is made. Joule heating flux q_j at the center of the wire-B ($x = 0$), which is the value per unit surface area converted from Q_j, is plotted in the figure. The heat transfer

curve q_c vs. T on the wire surface is also shown in the figure as a solid line. Furthermore, a vertical dotted line drawn in each figure is the critical temperature of the wire for the specified test current and magnetic flux density. The critical temperatures are 6.13 K under the condition for Fig. 4(a), and 5.77 K for Fig. 4(b), respectively.

Fig. 4(a) shows how to determine for the criterion for Group I. The Joule heating of the wire is less than the cooling on the surface of the wire after shutting off the heat input to the heater at $t = 20.00$ ms. The temperature of the wire decreases to the critical temperature of the wire where the cooling is still higher than the heating. The wire recovers to the superconducting state
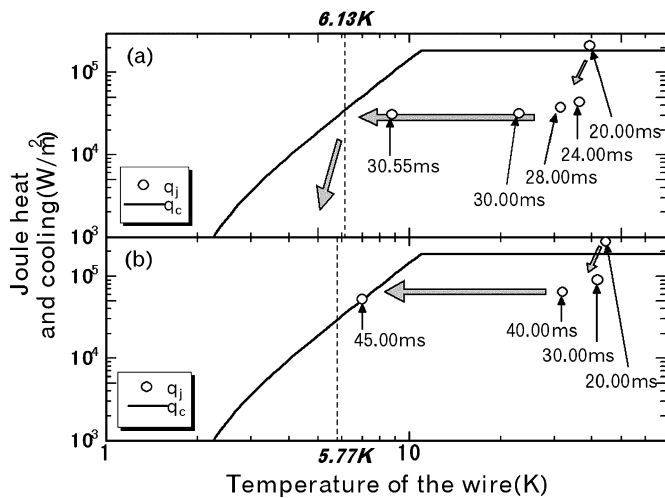
Fig. 4. Heat generation in the wire-B and heat transfer curve on wire-B surface belonging to (a) Group I ($T_b = 2.0$ K, $B = 4$ T, $I = 100$ A) and (b) Group II ($T_b = 2.0$ K, $B = 4$ T, $I = 130$ A).
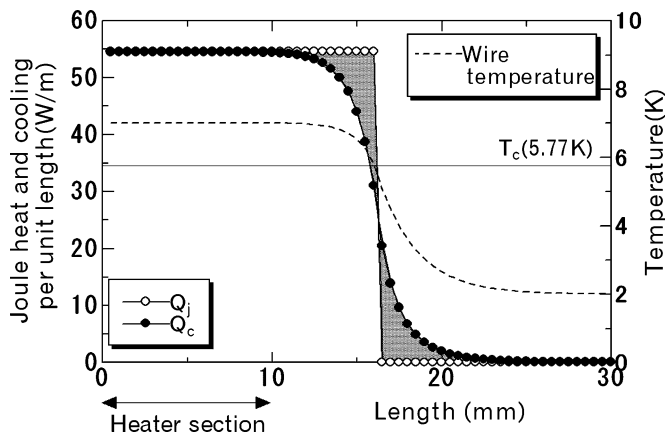

Fig. 5. Heat balance in a longitudinal direction of wire-B ($T_b = 2.0$ K, $B = 4$ T, $I = 130$ A).

as soon as the temperature becomes less than the critical temperature (6.13 K).

Fig. 4(b) is to explain the criterion for Group II. In this case too, the Joule heating of the wire is less than the cooling after shutting of the heat input, although the cooling at the heater shut off is in the film boiling regime. The temperature of the wire decreases and arrives at a point on the nonboiling curve at 45.00 ms, where Joule heating in the normal state is equal to the cooling on the surface. As the temperature of the central part is still higher than the critical temperature of the wire, the part of the wire doesn't recover to the superconducting state. Stationary normal zone remains. Fig. 5 shows the longitudinal heat balance for the final steady-state of Group II. The Joule heat and the cooling per unit length of wire-B are shown as open circles and solid circles, respectively. The distribution of the wire temperature and the critical temperature are also shown in the figure. Stationary normal zone exists in the left hand side of the figure where the wire temperature is higher than the critical temperature. In this range, the Joule heat is higher than the cooling. On the other hand, the Joule heat is zero and only cooling works in

the right hand side of the figure in superconducting state. The Joule heat and cooling heat flux integrated through the analyzed section (two shaded areas in Fig. 5) are equal. That is why the wire neither recovers to the superconducting state nor keeps increasing of the temperature. Group I or II is determined whether the temperature on the cooling curve corresponding to the Joule heating heat flux is lower or higher than the critical temperature, respectively.

In Group III, the temperature at the center of the wire keeps rising as shown in Fig. 1(c). The criterion for Group III is that the Joule heat in the part of normal zone is higher than the critical heat flux. The Joule heat becomes higher with increasing wire temperature but film boiling heat flux is almost constant for the temperature up to 100 K. As a result, wire temperature increases rapidly.

As shown in Figs. 3(a) and 3(b), the values of I_R are little affected by the variation of bath temperature. The critical temperature and Kapitza conductance, which have a lot to do with the criteria for Group I and Group II as mentioned above, hardly differ with the bath temperature. Therefore, the I_R is almost independent of the bath temperature. On the other hand, it is obvious that I_F is higher for the lower bath temperature. This is because the critical heat flux is involved in the criteria for I_F as mentioned above. The critical heat flux in pressurized He II is higher for lower bath temperature.

We can see in Fig. 3 that the experimental and numerical values of I_R for the wire-A with bare surface are higher than those for the wire-B with oxidized surface under the same condition. As the Kapitza conductance for the bare surface is higher than that for the oxidized surface, I_R of wire-A is higher than that of wire-B.

IV. CONCLUSION

The stability of the superconducting wire in pressurized He II has been analyzed using the one-dimensional model with the heat transfer database of He II. The results are in good agreement with the experimental data. We can argue over the stability of the superconducting wire with small diameter by using the one-dimensional model. From here onwards, it is concluded that the most important parameters that decide on the stability of the superconducting wire cooled by He II are Kapitza conductance on the wire and the critical heat flux in He II.

REFERENCES

[1] C. Meuris, B. Baudouy, D. Leroy, and B. Szeless, "Heat transfer in electrical insulation of LHC cables cooled with superfluid helium," *Cryogenics*, vol. 39, pp. 921–931, 1999.
[2] B. Baudouy, M. X. Francois, F.-P. Juster, and C. Meuris, "He II heat transfer through superconducting cables electrical insulation," *Cryogenics*, vol. 40, pp. 127–136, 2000.
[3] M. Ohya, S. Shigemasu, S. Shirai, M. Shiotsu, and S. Imagawa, Stability of Superconducting Wire With Various Surface Conditions in Pressurized He II (1) -Experimental Results-.
[4] A. Iwamoto, R. Maekawa, and T. Mito, "Kapitza conductance of the oxidized copper surface in saturated He II," *Cryogenics*, vol. 41, pp. 367–371, 2001.
[5] M. Shiotsu, K. Hata, and A. Sakurai, "Transient heat transfer for large stepwise heat inputs to a horizontal wire in subcooled He II," *Adv. Cryo. Eng.*, vol. 37A, pp. 37–46, 1991.